AIAA

A02-14192

AIAA 2002-0722

Micro Internal Combustion Swing Engine (MICSE) for Portable Power Generation Systems

W.J.A. Dahm, J. Ni, K. Mijit, R. Mayor, G. Qiao, A. Benajmin, Y. Gu, Y. Lei, and M. Papke

Laboratory for Turbulence & Combustion (LTC)
Department of Aerospace Engineering
The University of Michigan
Ann Arbor, MI 48109-2140

S.M. Wu Manufacturing Research Center (WuMRC)
Department of Mechanical Engineering
The University of Michigan
Ann Arbor, MI 48109-2125

Powerix Technologies, LLC
2600 Roseland, Suite 300
Ann Arbor, MI 48103-2135

Micro Internal Combustion Swing Engine (MICSE) for Portable Power Generation Systems

Werner J.A. Dahm[1,§], Jun Ni[2,*], Kevin Mijit[3,°], Rhett Mayor[2,∞], George Qiao[2,+],
Anish Benjamin[1,++], Yongxian Gu[1,++], Yong Lei[2,++], Melody Papke[2,++]

[1] *Laboratory for Turbulence & Combustion (LTC)*
Department of Aerospace Engineering
The University of Michigan
Ann Arbor, MI 48109-2140

[2] *S.M. Wu Manufacturing Research Center (WuMRC)*
Department of Mechanical Engineering
The University of Michigan
Ann Arbor, MI 48109-2125

[3] *Powerix Technologies, LLC*
2600 Roseland, Suite 300
Ann Arbor, MI 48103-2135

Recent progress is summarized in development of a palm-sized portable power generation system based on the micro internal combustion swing engine (MICSE). A swing engine is a rotationally oscillating free-piston engine in which combustion occurs in four chambers separated by a single rotating swing-arm, with virtually no other moving parts. The swing-arm creates four distinct combustion chambers in a single base structure; the resulting efficient use of both chamber space and system mass permits lower weight and smaller size at the same power than linear free-piston engines. The rotating swing-arm also produces less vibration than a linearly translating piston. The swing engine is unique among internal combustion systems in that it does not have any "dead point" in its operating cycle, and thus does not require an external starter. Mechanical-to-electrical power conversion is via a shaft-coupled inductive alternator outside the combustion chamber. The oscillating swing arrangement maintains a constant optimal separation between the magnets and inductive coil to provide more efficient coupling of mechanical power to electrical power. The swing motion produces excellent load-following characteristics; the system fully adjusts to large step changes in power demand in less than four swing cycles (0.05 sec). Load changes affect the swing angle more than the swing frequency, permitting system components to operate over a narrow range of frequencies for additional weight savings and increased reliability. Engine control requires only simple four-state bit logic based on threshold values of angular velocity obtained from the alternator output, and can be implemented without any mechanical linkage. Since timing is based on the swing-arm position, the system automatically adjusts to changes in external load, ambient temperature, and equivalence ratio. The engine currently under development is sized for 20W average electrical power output on butane fuel.

1. Introduction

Small-scale light-weight portable power generation systems that can convert the high energy densities available in liquid fuels into electrical power are emerging as a key leveraging technology for a number of critical aerospace-related application areas. Such applications range from micro air vehicles (MAV's) of various sizes, to robotic vehicles for various hazardous duty uses, to wearable computers for commercial and military uses, and to active power sources for portable electronics such as laptop computers and advanced wireless devices. Applications of this sort typically require power sources in the 1W to 100W range, with far higher specific energy and power than are achievable with current or foreseeable battery technologies. These applications and others like them thus depend critically on successful development of liquid-fueled "micro" power generation systems.

While fuel cells represent one promising approach toward the development of such small portable power generation systems, significant technical challenges remain in developing compact lightweight fuel reformers to permit fuel cells to operate with liquid hydrocarbon fuels. By contrast, internal combustion systems represent a comparatively mature technology for chemical power conversion, and dramatic reductions in the size of such

---

§ Professor of Aerospace Engineering. AIAA Associate Fellow. Head, Laboratory for Turbulence & Combustion (LTC). Corresponding author.

* Professor of Mechanical Engineering. Head, S.M. Wu Manufacturing Research Center.

∞ Postdoctoral Researcher.   + Research Scientist.   ++ Graduate Student.
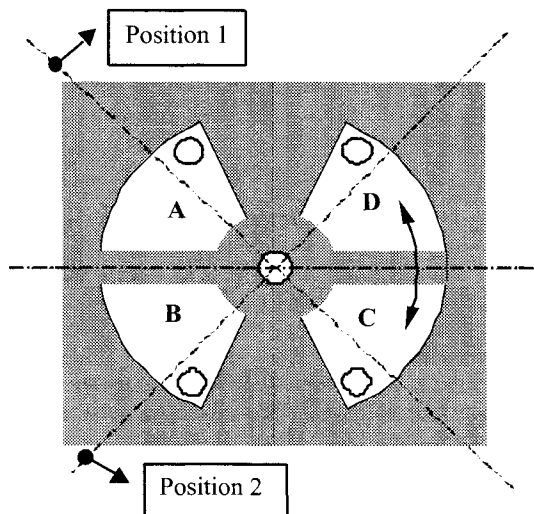
° Currently at Siemens Corporation.

systems have been demonstrated over the past five years by a number of research groups. The various micro engines currently under development in these efforts can be grouped by the thermodynamic cycle on which they are based (e.g., Brayton, Rankine, Stirling, Otto). The micro gas turbine effort at MIT has received the most attention, though the inherently short residence times available for combustion in such a system would appear to restrict its use to gaseous hydrogen fuel, for which fuel cells are the clear technology-of-choice. Other internal combustion engine development efforts currently underway include the micro Wankel engine (UC Berkeley), as well as several linear free-piston engines, including a micro free-piston knock engine (Honeywell), a planar free-piston engine (Georgia Tech), and a single-ended free-piston engine (Aerodyne).

A Micro Internal Combustion Swing Engine (MICSE) is an innovative internal combustion device for chemical-to-mechanical energy conversion that is potentially suitable for such a micro power generation system. The operating principle is described in detail in §2. Briefly, a swing engine is a rotationally oscillating free-piston engine in which combustion occurs in four chambers separated by a single rotating swing-arm, with virtually no other moving parts. This swing-arm creates four distinct combustion chambers in a single base structure. Due to the resulting efficient use of both chamber space and system mass, the swing engine permits lower weight and smaller size at the same power than linear free-piston engines. The low mass, low moment of inertia, and angular motion of the rotationally oscillating swing-arm also produce less vibration than a linearly translating piston. The swing engine is further unique among internal combustion systems in that it does not have any "dead point" in its operating cycle, and thus does not require an external starter. The MICSE system functions on an Otto cycle, but is otherwise fundamentally different from the various linear piston engines noted above. Furthermore, while the MICSE system involves a rotating piston

motion, it is completely different from rotary engines like the Wankel noted above. Conversion of the mechanical power produced by the engine to electrical power is via an inductive alternator, either with permanent magnets in the swing arm and inductive coils in the cavity base, or by an external shaft-coupled inductive alternator optimized for the rotationally oscillating motion produced by the swing engine.

The swing engine concept itself is not new; the earliest patents related to swing engines date to the early 1900's. However, prior work has sought to develop the swing engine as mechanical power source. These efforts have met with little practical interest, since there is essentially no demand for the inherently oscillating shaft power that is produced by a swing engine. Other work has sought to develop mechanical transmissions to covert this oscillating shaft motion into a continuous rotating motion, but such systems are too complex for most practical uses. As a result, while swing engines have inherent weight and volume advantages over linear piston engines, yet they are not well suited as mechanical power sources.

In contrast, this effort is the first to examine the swing engine as the basis for an electrical power source, in which the rotationally oscillating swing arm motion drives an alternator that converts the mechanical power into electrical power. The swing engine turns out to have a number of features that make it exceedingly well-suited as an electrical power generator. The swing-arm maintains a constant optimal separation between the magnets and inductive coil to provide efficient coupling of mechanical power to electrical power. The swing motion produces excellent load-following characteristics; the system fully adjusts to large step changes in power demand in less than four swing cycles (0.05 sec). Load changes principally affect the swing angle rather than the swing frequency, permitting system components to operate over a narrow range of frequencies, providing for additional weight savings and increased reliability. Engine control requires only simple four-state bit logic using threshold angular velocities obtained from the alternator output, and can be implemented in a chip without any mechanical linkage. Since timing control is based on the swing-arm position, the system automatically adjusts to changes in external load, equivalence ratio, and other operating factors. The inherently fast system response time (0.05 sec) allows for virtually immediate on-demand startup and shutdown from the engine control circuit.

This paper summarizes the principles involved in swing engine design, and describes a 65W benchtop-scale MICSE system with complete external engine control system that has been built and tested at Michigan. It also describes recent progress in developing a palm-scale MICSE system for 20W average power output. This system is being integrated in a complete power generation system with a projected mass of approximately 54 g (non-fuel) and occupying approximately 17 cm³ volume. The system is designed to operate at 102.8 Hz with a thermal efficiency of 14.4% and 12.8% parasitic losses, to produce 37.2W of mechanical power and 21.1W of net electrical power.


Figure 1. Base cavity, swing-arm, valve ports, and resulting four chambers (A-D) in the micro internal combustion swing engine (MICSE). The resulting arrangement produces inherent weight and volume efficiencies over conventional linear piston engines, while avoiding the mechanical complexities of rotary Wankel or turbine engines. Two- and four-stroke implementations are possible.

2. Swing Engine Operating Principle

It is the swing engine itself (see Figs. 1 and 2) that is the prime innovation in the MICSE approach, and that provides many operational advantages over other micro power generation devices, including linear piston engines, rotary Wankel engines, and mi-
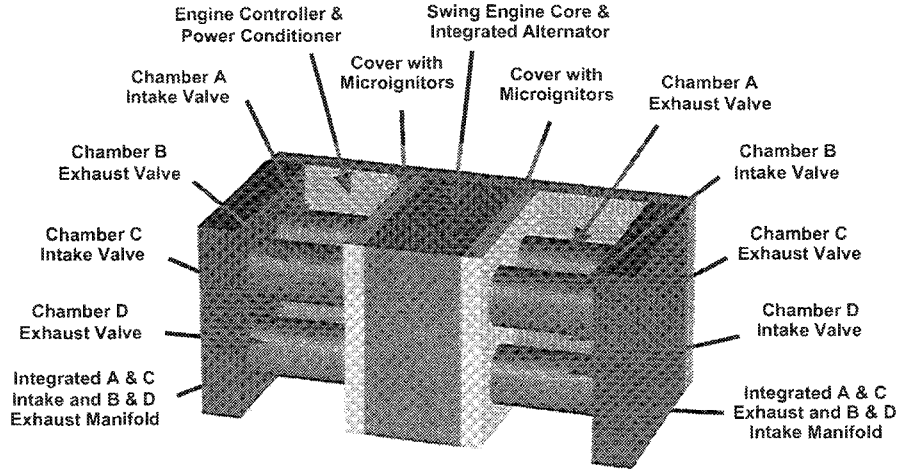
Figure 2. Assembly concept for all non-fuel components of the 20W MICSE chemical-to-electrical energy conversion system, indicating major system components. System volume is 17.6 cc ($20\times20\times44$ mm^3) and mass is 54 g.

croturbines. A swing-arm divides the engine base cavity into four distinct chambers (A-D), effectively collapsing the four cylinders of a conventional piston engine into a single base structure. The resulting mass and volume efficiencies that this produces allow for far lower weight and smaller size, at the same power, than any conventional linear piston approach.

As the center-swing in Fig. 1 rotates around its pivot, it produces in a single motion the same intake, compression, combustion and exhaust strokes required by any internal combustion engine. For example, when the swing-arm is rotating toward Position 1, the volume decreases in chambers A and C and increases in chambers B and D. By keeping open the intake valve on B and the exhaust valve on C, and triggering the ignitor on D, the result is that A is in its compression stroke, B in its intake stroke, C in its exhaust stroke, and D in its combustion stroke. The angular motion of the swing-arm decreases as chamber A is further compressed, and eventually stops when the swing arm is at a final "clearance angle" from the cavity end wall, at which A reaches its maximum compression.

At this point, the valve states are changed to open the exhaust on D and the intake on C, and the microignitor in A is triggered. The swing-arm then rotates in the opposite direction due to the high pressure and the large heat added by combustion in A. The swing-arm repeats a similar motion as before, but with the new valve states changing the intake, compression, combustion and exhaust chambers, and eventually stops at the clearance angle from the other cavity end wall. The result is that the swing arm rotates back and forth, with cyclic valve and ignitor states. Power is continuously provided by combustion occurring in one of the chambers during each quarter-cycle of the engine, in contrast to single-chamber or two-chamber linear piston engines.

In addition to such four-stroke operation, the swing engine can also be operated on a two-stroke cycle. In this case, chambers A and C are always at the same state, as are chambers B and D. The active exhaust valves implied in the four-stroke operation are then replaced with simple exhaust ports in the engine cover

plates, as shown in Fig. 3. As the swing arm moves under the combustion pressure in chambers A and C, it eventually clears to exhaust port and allows the remaining high-pressure combustion products to vent. Inflow of fresh premixed fuel-air charge begins as the intake valve is opened when the pressure is chambers A and C drops, and serves to scavenge remaining combustion products from these chambers as the swing arm reverses its motion. When the swing arm closes the exhaust port on its return motion, inflow of the premixed reactants stops as the pressure rise closes the intake valves. Further motion of the swing arm serves to compress the fuel-air charge until the swing arm stops at the clearance angle from the cavity wall. At this point, the ignitors on A and C are triggered, and the cycle repeats, with the same processes occurring out of phase in chambers B and D. In this case, there are two power strokes per cycle, with an attendant increase in power density, but with the usual nominal reduction in thermal efficiency.

3. MICSE System Design and Performance Model

It is possible to determine the performance of both a four-stroke and a two-stroke MICSE system by a detailed system design model that includes the detailed engine part geometries and masses, the system dynamics including the counter-torque from the inductive alternator, detailed gas dynamics of the intake and exhaust processes, and detailed thermodynamics of the compression and expansion processes.

Consider first the four-stroke cycle. Assuming that chamber A is on its intake stroke, chamber B on its exhaust stroke, chamber C on its combustion stroke, and chamber D on its compression stroke, then the swing arm angular acceleration $d^2\theta/dt^2$ can be expressed as

$$\frac{d^2\theta}{dt^2} = \frac{(p_C + p_A - p_B - p_D)A_S L_A - T_r}{I} \tag{1}$$

where p_C and p_A are, respectively, the combustion chamber pressure (driving pressure) and the intake chamber pressure, and p_B and p_D are the exhaust chamber pressure and compression

Exhaust ports open for A and C   Exhaust port closed   Exhaust ports open for B and D
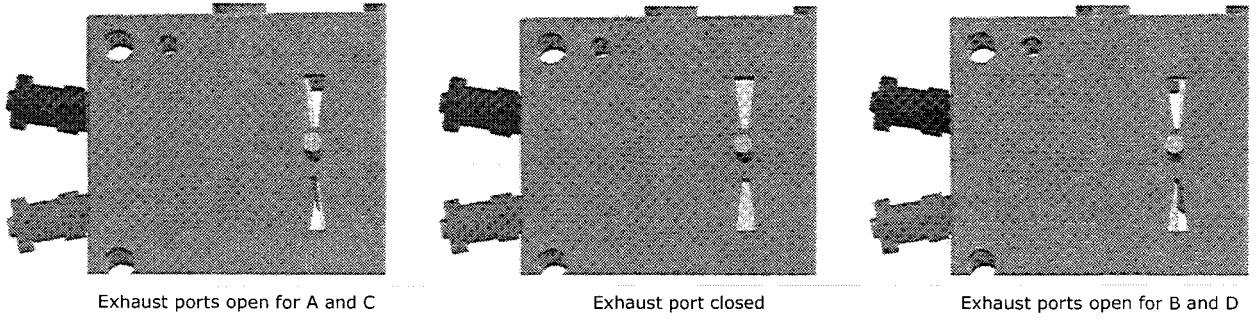
Figure 3. Two-stroke MICSE system, showing exhaust ports in engine cover plates, and effect of swing arm position relative to port geometry. The two-stroke version eliminates the need for high-temperature active exhaust valves.

chamber pressure (load pressures), A_S is the arm area of the center-swing, L_A is the distance from the driving force working point to the pivot, determined by the swing arm geometry, I is the angular inertia of the center-swing assembly, which includes the effect of any external mass, and T_r is the external torque resulting from the torque induced by the inductive power generation system and any friction forces between matching surfaces.

When there is an external electrical load that is consuming energy generated from the MICSE, then the external torque T_r will be the sum of the induced resistive torque from generator and from friction within the engine as

$$T_r = \frac{B^2 L^2 r_s^2}{R_l}\dot{\theta} + T_f \qquad (2)$$

where B is the strength of the magnetic field of the inductive generator, L is the length of the conductor (coil), r_s is the rotor radius, $d\theta/dt$ is the angular velocity of the swing arm, and R_l is the external electrical load, with T_f being the resistive torque due to friction on the swing arm surfaces.

The temperature and pressure inside each chamber can be expressed as

$$\dot{T} = \frac{RT}{C_v}\left[\dot{x}_b\left(\frac{R_b - R_u}{R} + \frac{h_b - h_u}{RT}\right) + \frac{\dot{m}}{m} - \frac{\dot{V}}{V}\right]$$
$$+ \frac{1}{mC_v}\left[\sum_i \dot{m}_i h_i - \dot{Q}_w\right] \qquad (3)$$

and

$$\dot{p} = p\left[\dot{x}_b\frac{R_b - R_u}{R} + \frac{\dot{T}}{T} + \frac{\dot{m}}{m} - \frac{\dot{V}}{V}\right] \qquad (4)$$

where $p(t)$ is the pressure in the chamber, $V(t)$ is the volume of the chamber, Q_w represents the heat transfer losses, $m_j(t)$ and $h_j(t)$ are the mass and specific enthalpy of the flows into or out of the chamber, $R(t)$ represents the value of the gas constant for the mixture inside the chamber, $T(t)$ is the temperature, and $x_b(t)$ is the burned mass fraction.

From the base cavity geometry, the volume $V(t)$ of each chamber can be expressed in terms of the respective individual part dimensions as

$$V = \frac{h_b(\phi/2 - \theta)}{2}\left(R_b^2 - r_b^2\right) - \frac{h_b t_b}{2}\left(R_b - r_b\right) \qquad (5)$$

where t_b is the swing-arm thickness, and R_b and r_b are, respectively, the base radius and hinge radius of the MICSE base structure. The first term in (5) thus represents the volume enclosed by the center plane of the swing arm, the surfaces of the base cavity wall, the hinge, and the top and bottom covers, and the second term is the volume occupied by the swing arm.

Conservation of mass inside each chamber is given by

$$\frac{dm}{dt} = \frac{c_d A p_0}{\sqrt{RT_0}}\left(\frac{p_s}{p_0}\right)^{1/\gamma}\left\{\frac{2\gamma}{\gamma-1}\left[1 - \left(\frac{p_s}{p_0}\right)^{\frac{\gamma-1}{\gamma}}\right]\right\}^{1/2} \qquad (6a)$$
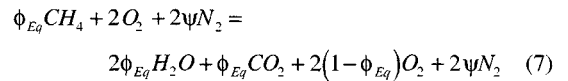
or, if the flow, entering or exiting the chamber is choked, then is given by

$$\frac{dm}{dt} = \frac{c_d A p_0}{\sqrt{RT_0}}\gamma^{1/2}\left(\frac{p_s}{p_0}\right)^{1/\gamma}\left(\frac{2\gamma}{\gamma-1}\right)^{\frac{\gamma+1}{2(\gamma-1)}} \qquad (6b)$$

where A is the port inflow/outflow area, c_d is the discharge coefficient, γ is the ratio of specific heats, p_0 and T_0 are the stagnation pressure and temperature, and p_s is the static pressure at the restriction.

For any specified fuel, all necessary mixture properties in (3) and (4) can be found. Then after specifying the burned mass fraction $x_b(t)$ using a Wiebe function and recursively-applying (3) - (6) for each individual cycle, the time-varying temperature $T(t)$ and pressure $p(t)$ inside all the chambers can be determined, giving the swing angle $\theta(t)$ from (1) and (2).

Thus, for example, for a lean mixture of methane and air at equivalence ratio ϕ_{Eq}, the overall reaction can be written as

$$\phi_{Eq}CH_4 + 2O_2 + 2\psi N_2 =$$
$$2\phi_{Eq}H_2O + \phi_{Eq}CO_2 + 2\left(1 - \phi_{Eq}\right)O_2 + 2\psi N_2 \qquad (7)$$

where ψ is the molar ratio of N_2/O_2; for pure air ψ is 3.773. Specifying the burned mass fraction with a standard Wiebe function as

$$x_b = 1 - x_{u0}e^{-a\left(\frac{t}{\tau_b}\right)^{m+1}} \qquad (8)$$
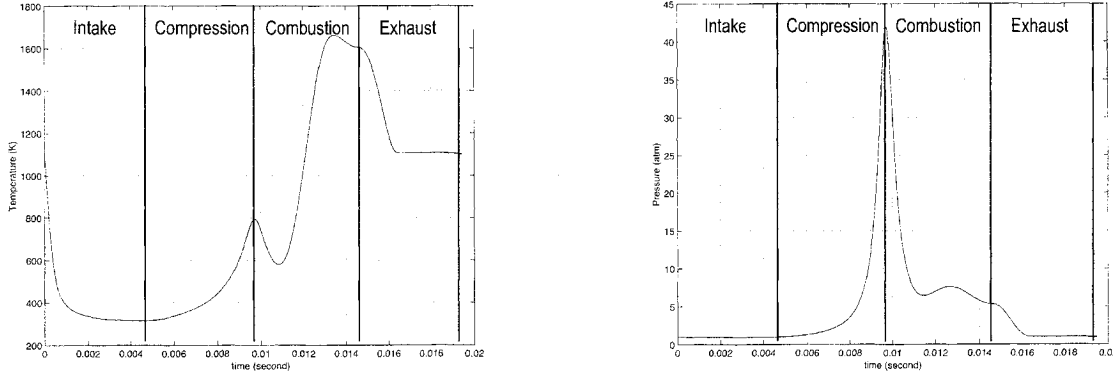
Figure 4. Chamber temperature *(left)* and pressure *(right)* versus time over one full cycle of the 20W small-scale MICSE swing engine operating on butane fuel, from the simulation procedure in §3. System performance characteristics are given in Table 1.
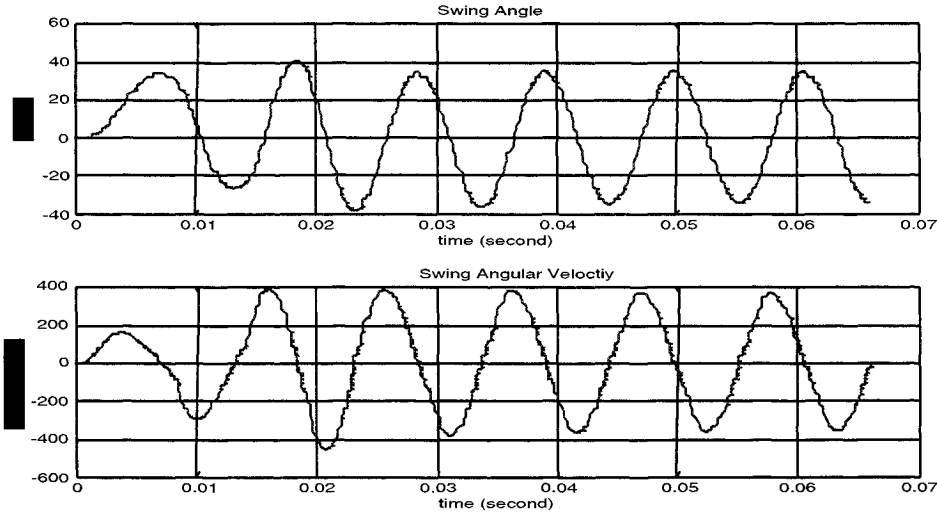
Figure 5. Cold start simulations of MICSE system, verifying that lack of "dead points" in swing engine cycle allows startup from remaining lean charge in at least one chamber. Steady state oscillation is reached after less than five swing cycles, corresponding to less than 0.05 sec.

gives the major species concentrations in terms of $x_b(t)$ as

$$f_{CH_4} = \frac{16\phi_{Eq}(1-x_b)}{16\phi_{Eq}+64+56.32\,\psi}$$ (9a)

$$f_{O_2} = \frac{64(1-\phi_{Eq}x_b)}{16\phi_{Eq}+64+56.32\,\psi}$$ (9b)

$$f_{N_2} = \frac{56.32\,\psi}{16\phi_{Eq}+64+56.32\,\psi}$$ (9c)

$$f_{CO_2} = \frac{44\phi_{Eq}}{16\phi_{Eq}+64+56.32\,\psi}$$ (9d)

$$f_{H_2O} = \frac{36\phi_{Eq}x_b}{16\phi_{Eq}+64+56.32\,\psi}$$ (9e)

From the known time-varying species concentrations, the specific heats follow as

$$c_{p,i} = \left(a_{i1}+a_{i2}T+a_{i3}T^2+a_{i4}T^3+a_{i5}T^4\right)R_i$$ (10)

and the enthalpies as

$$h_i = \left(a_{i1}+\frac{a_{i2}}{2}T+\frac{a_{i3}}{3}T^2+\frac{a_{i4}}{4}T^3+\frac{a_{i5}}{5}T^4+\frac{a_{i6}}{T}\right)R_iT$$ (11)

with the mixture properties then being

$$h = \sum f_i h_i$$ (12a)

$$c_p = \sum f_i c_{p,i}$$ (12b)

$$c_v = \sum f_i c_{v,i}$$ (12c)

The resulting system can thus be integrated forward in time to provide the pressure $p(t)$ and temperature $T(t)$ in each chamber as a function of time. Such results are shown for a 20W-scale
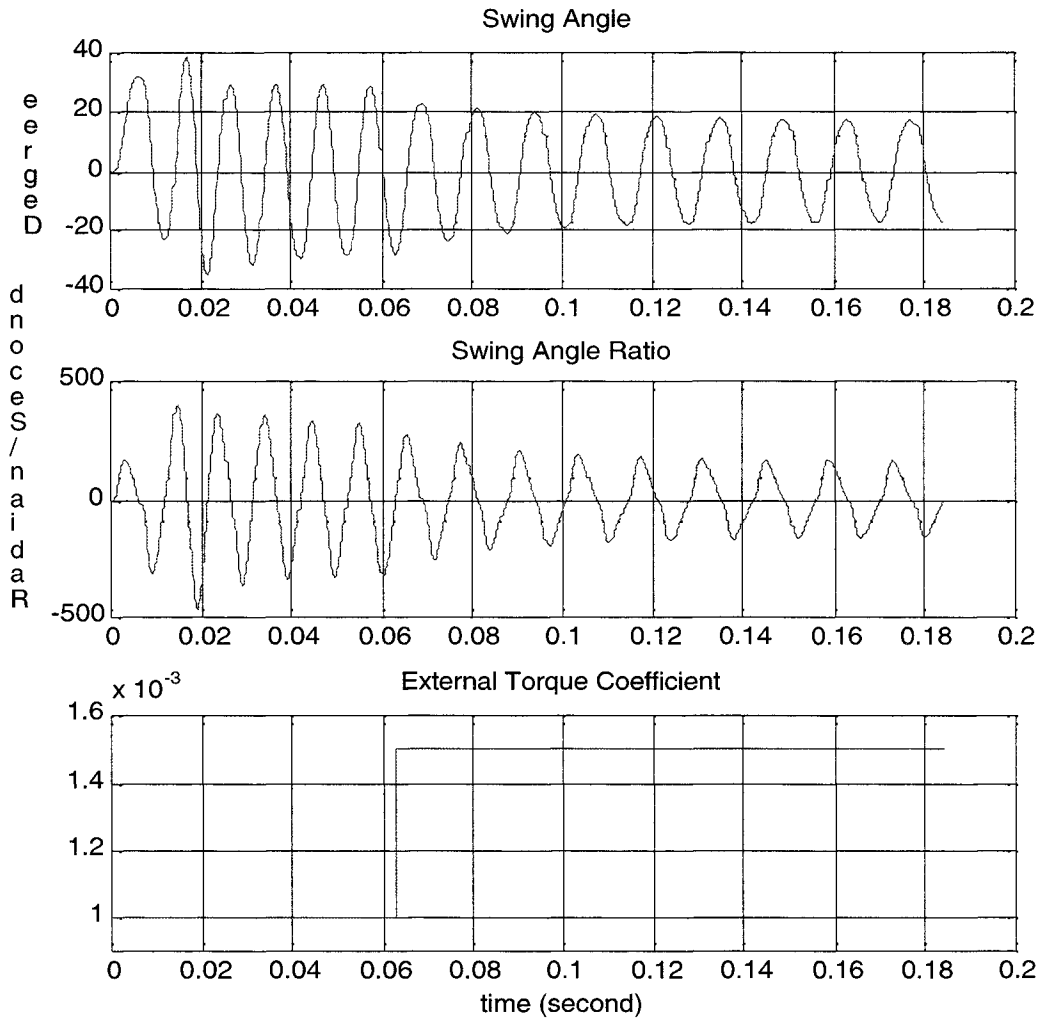
Swing Angle

Swing Angle Ratio

External Torque Coefficient

Figure 6. Swing engine response to a 50% step increase in electrical load shortly after startup transient. The inherently oscillatory nature of the swing engine allows the system to rapidly adjust to the new operating point (swing angle and swing frequency).
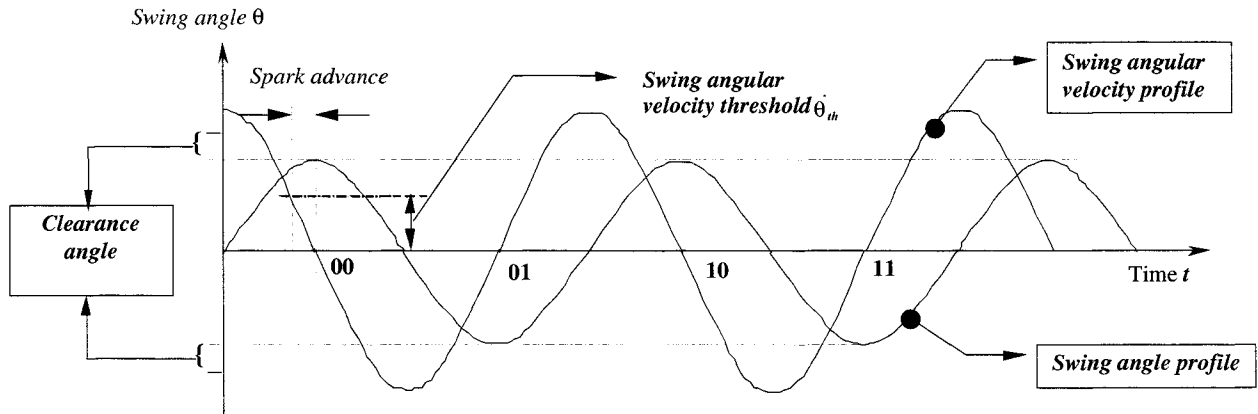
Figure 7. Clearance angle detection in the MICSE control scheme.

• Fuel	Butane vapor, 300 K, 1atm
• Consumption rate	1.81 (10^{-5}) g/stroke
• Consumption per hour	13.33 g
• Oxidizer	Air, 300 K, 1 atm
• Consumption rate	5.87 (10^{-4}) g/stroke
• Consumption per hour	434.5 g
• Air-fuel mass ratio	32.6 : 1
• Stoichiometric A/F ratio	15.4 : 1
• Equivalence ratio	2.11
• Flame speed	87 cm/s
• Intake port diameters	2 mm
• Intake valve clear $\varnothing$	> 2 mm
• Exhaust port diameters	2 mm
• Exhaust valve clear $\varnothing$	> 2 mm
• Port discharge coefficient	50%
• Valve open/close time	1 ms
• Combustion duration	4 ms
• Ignition timing	$0°$ BTC
• Clearance angle	$6.77°$
• Swing engine mass	30.6 g
• Cycle speed	102.8 Hz
• Gross work/cycle	0.181 J
• Pumping work/cycle	0.029 J
• Net work/cycle	0.152 J
• Specific fuel consump.	358.4 g/kWh
• Thermal efficiency	21.9%
• Mechanical power	37.20 W
• Inductive efficiency	65%
• Parasitic losses	3.1 W
• Net electrical power	21.1 W

Table 1. Steady state performance characteristics of 20W MICSE swing engine operating on butane fuel..

Figure 8. 65W benchtop-scale MICSE 0 assembled for initial testing of swing engine power generation system, showing swing engine with cover removed *(top)* and fully assembled engine *(bottom)*. Fabrication was done to 10 μm tolerance with wire EDM. Large-scale automotive spark plugs were used for ignition. Reed valves were used on intake side, and large-scale solenoid valves on exhaust side.

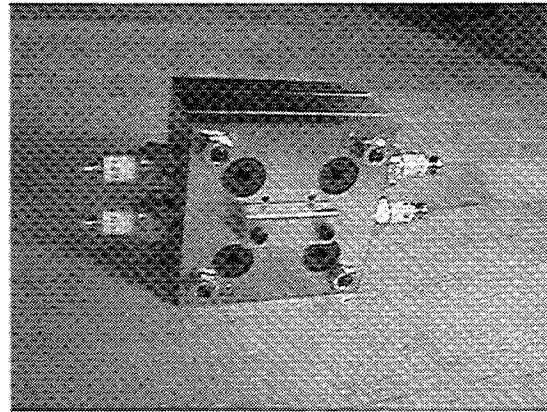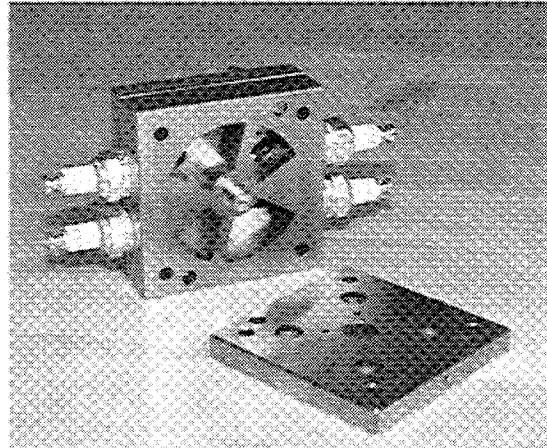MICSE system in Fig. 4, where the intake, compression, combustion, and exhaust strokes are indicated.

For a two-stroke cycle the procedure above is the same, except that (1) is replaced by

$$\frac{d^2\theta}{dt^2} = \frac{2(p_A - p_B)A_s L_A - T_r}{I} \qquad (13)$$

and outflow process begins when the swing arm begins to clear the exhaust port.

4. MICSE System Operational Characteristics

This section presents the major operating characteristics of a MICSE power generation system as inferred from detailed simulations of the type described in §3. These provide quantitative assessments of startup capability, steady state operating characteristics, load-following capability, and shutdown characteristics. It turns out that the major operating characteristics of a MICSE system do not change dramatically with the power level for which the swing engine is designed. The results are present-

ed here are applicable to both the 65W benchtop scale system and the 20W palm-sized system currently being developed.

4.1 Startup

Cold start can be a difficult issue for most IC-based approaches to portable power generation. However, the swing-engine principle on which the MICSE system is based is unique among IC-approaches in that it does not have any "dead point" in its operating cycle that must be overcome by accumulated inertia. (Such "dead points" are the reason why automobile engines must have a starter motor.) For this reason, the MICSE system does not need any starter and does not need to be manually primed. The engine may be readily started by igniting the fuel-air charge left in at least one cylinder from the previous shutdown. This has been confirmed using detailed simulations of the startup process, in which one cylinder was left charged with a (lean) fuel-air equivalence ratio of 0.3. Results for start-up of such a swing engine with an integrated alternator simulation are shown in Fig. 5, where it is apparent that the steady state oscillation is already approached on the second swing cycle, and is fully achieved
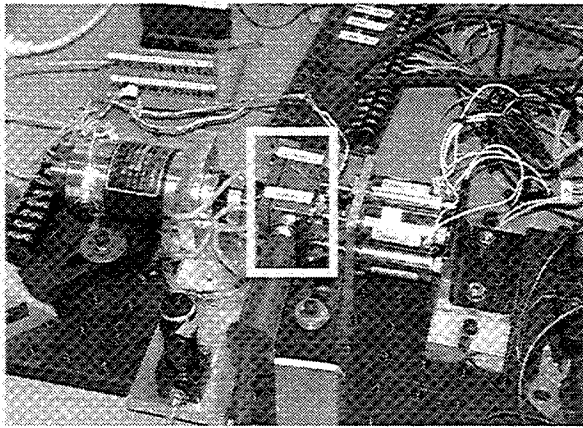
Figure 9. Photograph of test arrangement for 65W benchtop-scale MICSE 0, showing fully-assembled swing engine *(insert)* with solenoid valves *(right)*, external shaft-coupled inductive alternator *(left)*, fuel proportioning valve *(bottom)*, and spark plug wires *(top and bottom)*. Engine control was via PC-in-the-loop arrangement. Note that all components in this benchtop-scale system are being reduced to meso- and micro-scale in the complete 20W palm-sized MICSE power generation system under development.
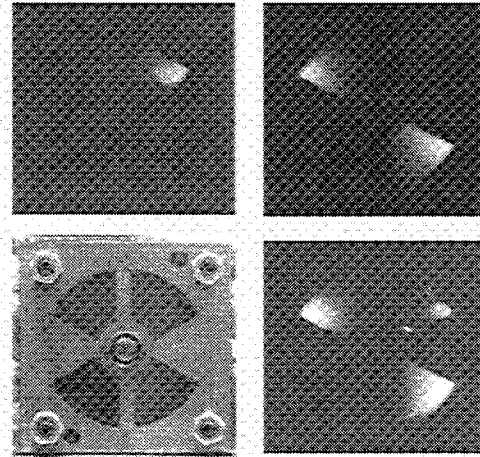
Figure 10. Photographs of combustion in 65W benchtop-scale MICSE 0 showing engine with front cover replaced by glass to permit visualization *(bottom left)*, and direct photographs with ignition in one, two, and three combustion chambers. Ignitor location is in corner of each chamber.

within five cycles, corresponding to less than 0.05 sec. This fast response is due to the low moment of inertia of the swing arm, and the fact that the swing engine has no "dead point" in its cycle where accumulated inertia must be relied on to continue the cycle. The ease with which a MICSE system can be cold-started is one of several major advantages of this approach.

4.2   Load Following

Changes in the electrical demand on the system produce a change in the inductive torque produced by the alternator that resists the swing arm motion. In a swing engine, the clearance angle simply adjusts to the new operating point dictated by the induced torque coefficient. Moreover, this change occurs very rapidly, as seen in the simulation results in Fig. 6, showing the system response to a 50% step increase in electrical load being drawn from the alternator. The system fully adjusts to the new swing angle and frequency over about four swing cycles (*i.e.*, a time of about 0.05 sec). As a result, the MICSE system should follow load changes that occur on time scales slower than this. Note also in Fig. 5 that the resulting change in engine operation due to this change in electrical load is mainly in the swing angle rather than the swing frequency, allowing valves and other system components to be designed for a relatively narrow range of operating frequencies.

4.3   Shutdown

The MICSE power generation system can be readily shutdown via the engine control system by simply interrupting the spark provided by the microignitors. For the small-scale system this responds on a time scale of about 0.05 sec, allowing virtually immediate shutdown on demand. Moreover, after the ignition has been interrupted, the remaining swing motion rapidly damps out, and in doing so draws fresh fuel-air mixture into each of the four chambers. This provides the residual charge needed to

restart the system, without any need for manual priming.

4.4   Engine Control

The engine control circuit for a MICSE system principally provides trigger signals for the intake and exhaust valves and for the igniters. These are generated relative to the swing-arm angular position implied by the voltage output of the inductive alternator. The angular velocity is directly proportional to the voltage generated. As a result, the zero-voltage crossover point indicates the swing arm end position (clearance angle). Figure 6 defines a "zero-crossover comparison threshold" used to set the spark advance to control the peak pressure in the combustion process. Since the center-swing frequency is twice that of the control state, the required control state can be determined by the swing-arm position and the previous control state. Because there are only four different control states, the previous state is stored as a two-bit number and the corresponding new control stored in a look-up table. On startup, the system initializes the binary counter to 00 and sets chamber A exhaust to open. At the next zero-threshold crossing, the binary counter is incremented by one and the next control action is triggered from the look-up table. The system thus automatically adjusts to changes in the swing-arm frequency during load changes or startup.

4.4   20W MICSE Operating Characteristics

Table 1 shows the major operating characteristics of a 20W four-stroke MICSE power generation system, as obtained from this detailed system simulation procedure. The system was designed to operate on butane fuel, with the equivalence ratio set very lean to keep the combustion product temperatures relatively low. This allows the active exhaust valves in the four-stroke engine to be exposed to the lowest temperatures possible, but imposes a thermal efficiency penalty on the system. Of key interest is that the engine operating cycle is approximately 100 Hz, with a clear-
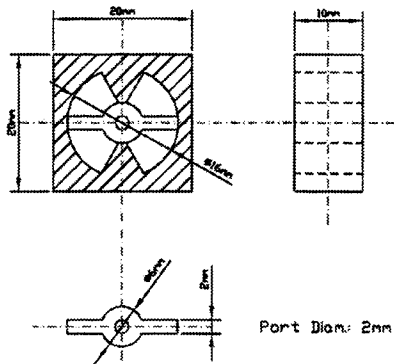
Figure 11. Dimensions of initial 20W palm-sized MICSE core, showing 16 mm cavity in 20 × 20 × 10 mm block.

ance angle of just under 7-degrees. Note that approximately 15% of the work per cycle goes into pumping losses due to the relatively small intake and exhaust port sizes. This imposes another efficiency penalty on the system. Note also that both of these efficiency penalties would not occur in a two-stroke system, where there are no active exhaust valves and thus near-stoichiometric operation is possible with much lower pump losses across the comparatively large exhaust ports.

5. Benchtop-Scale MICSE System Testing

A benchtop-scale four-stroke MICSE system, designated MICSE 0, was fabricated and tested at The University of Michigan. Design of the system was based on the detailed system model outlined above. The system was sized for 65 W-scale operation, and used hydrogen and methane as fuels. The swing engine core, shown in Fig. 8, measured 61 × 61 × 34 mm and was fabricated from steel with wire EDM techniques. Very tight tolerances on the gaps between the swing-arm tip and the engine body, and between the top and bottom surfaces of the swing arm and the corresponding engine cover plates, allowed operation without any seals. The resulting gap sizes were roughly 10 μm, and provided completely adequate sealing between chambers.

The test arrangement is shown in Fig. 9. Commercially-available components were used at this initial stage of development for several key parts of the system, since minimizing weight and volume were not the main goals of the initial test program. For this reason, intake valves were simple flippers made of spring steel, which were deflected by the negative pressure during the intake stroke. Exhaust valves were conventional spring-loaded push-rod solenoids, and conventional automotive spark plugs were used for spark ignition. For diagnostic purposes, temperatures in each of the four combustion chambers were measured with wall-mounted thermocouples. A permanent magnet DC tachometer coupled to the swing engine output shaft functioned as an alternator for electrical power generation. The engine was integrated with a complete PC-based engine control system that measured the swing-arm angular position from the output of the power generator, and provided actuation signals for the exhaust valves and the spark plugs. This control system was successfully used to cold-start the benchtop MICSE unit.
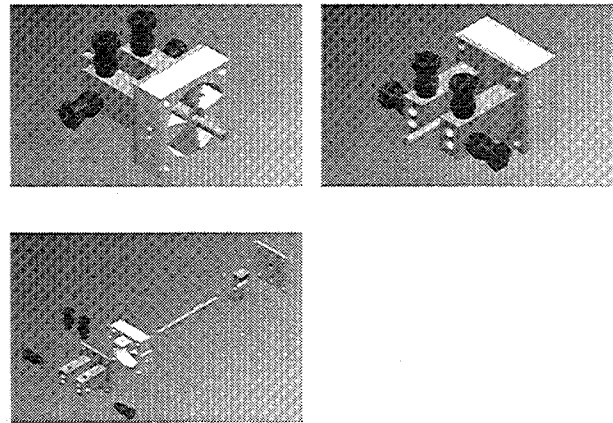

Figure 12. Conceptual design of 20W palm-sized MICSE core, showing cavity block, swing arm, shaft, back cover plate, intake valves and fittings. This design is for two-stroke operation to eliminate high-temperature exhaust microvalves.
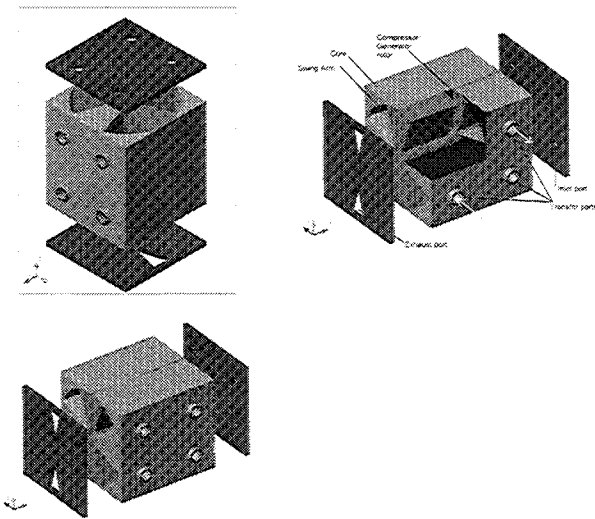

Figure 13. Conceptual design of supercharged two-stroke 20W palm-sized MICSE core, showing same engine core as above but with second swing core serving as precompression section. Permanent magnets and coils for inductive alternator are integrated in swing arm and cavity walls on supercharger side, where temperatures are comparatively low.
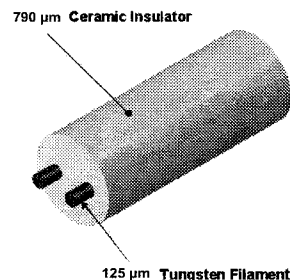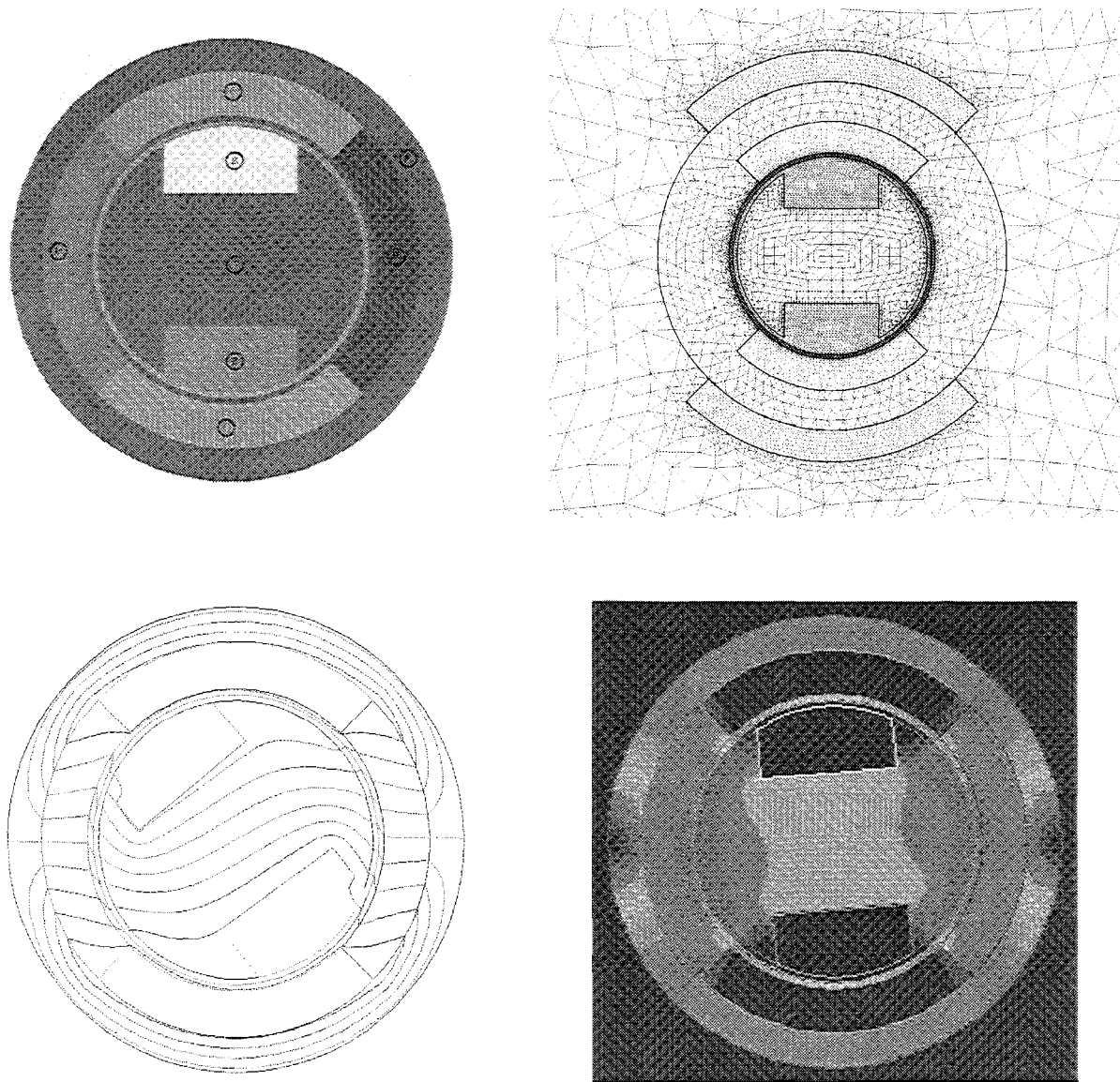

790 μm **Ceramic Insulator**

125 μm **Tungsten Filament**

Figure 14. Microignitors developed for palm-sized MICSE power generation systems, consisting of 790 μm commercial ceramic thermocouple insulator and 125 μm tungsten filaments.

Figure 15. Electromagnetic simulations of an inductive alternator design, performed using Maxwell 2D™ and EM Pulse™, showing alternator layout *(top left)* with permanent magnets, coil with specified number of windings and load resistance, salient magnetic loop of specified material, and air gaps. A typical grid for such simulations is shown *(top right)*, with resulting instantaneous magnetic flux lines *(bottom left)* and flux density field *(bottom right)*. Parametric simulations include all magnetic saturation effects, and allow specified variation in swing arm angle with time.

More than 1200 tests were conducted on this initial MICSE system, in which a total of 694-liters of hydrogen fuel and 158-liters of methane fuel were burned. The testing varied the fuel type, fuel-air mixture ratio, valve timing, spark ignition timing, and other parameters to examine their effect on the system performance and allow comparisons with the detailed system model. Figure 10 shows combustion in the swing engine chambers during cold-start operation, with one of the covers replaced by a window for visualization purposes. These tests showed that operation of a MICSE system for small-scale power genera-

tion could be done, and studied the effect of various configuration and operating parameters on the engine.

6. Small-Scale MICSE System Performance

The simulation methodology in §3 was used to design a MICSE swing engine for a 20W power generation system operating on butane fuel. The resulting swing engine core dimensions are shown in Fig. 11, with the associate four-stroke operating characteristics given in Table 1. From these, detailed design and operating information were obtained and the system performance

System Component (Quantity)	Weight (g)		Volume (cm^3)		Power (W)	
	Current	Achievable	Current	Achievable	Current	Achievable
Swing engine cavity[1] (1)	18.3	15	4.0	4.0	+37.2	+37.2
Swing arm[1,8] (1)	2.4	2.0	---	---	---	---
Swing arm bearings[1,9] (2)	2 × 0.4	2 × 0.4	---	---	---	---
Left cover[1] (1)	1.6	1.2	0.4	0.3	---	---
Right cover[1] (1)	1.6	1.2	0.4	0.3	---	---
Intake valves[2] (4)	4 × 2.5	4 × 0.3[10]	4 × 0.4	4 × 0.1	(4 × 0.3)	0
Exhaust valves[2] (4)	4 × 2.5	4 × 2.5	4 × 0.4	4 × 0.4	(4 × 0.3)	(4 × 0.3)
Microignitors[3,4] (8)	0.2	0.2	~ 0	~ 0	(0.4)	(0.4)
Engine control circuit[3] (1)	1.6	1.6	3.0	3.0	(0.1)	(0.1)
Internal battery[3,5] (1)	0.5	0.5	0.2	0.2	(~ 0)	(~ 0)
Integrated manifolds[3] (2)	2 × 1.8	2 × 1	2.0	2.0	---	---
Fuel tank interconnect[3] (1)	0.8	0.8	0.1	0.1	---	---
Fuel lines[3] (1)	1.2	1	0.3	0.3	---	---
Permanent magnets[6] (2)	---	---	---	---	---	---
Inductive coils[7]	---	---	---	---	(13.0)	(13.0)
Power conditioner[3] (1)	1.6	1.6	3.0	3.0	(0.2)	(0.2)
Power terminals[3] (2)	0.15	0.15	0.1	0.1	---	---
	54.4 g	**39.3 g**	**16.7 cm^3**	**15.3 cm^3**	**21.1 W**	**22.3 W**
JP-8 microvaporizer[2] (1)	6	4	0.6	0.6	---	---
Butane preheat reservoir[3] (1)	0.4	0.3	0.01	0.01	---	---

[1] Actual value based on current state-of-the-art
[2] Projected values from subcontractor estimates
[3] Estimated value based on preliminary design and available information
[4] Combined weight of 8 microignitors
[5] Typical high pulse 1.5V rechargeable Zn/MnO_2 (Eveready Type 192)
[6] Displaces weight and volume already accounted for in swing arm
[7] Displaces weight already accounted for in swing engine cavity
[8] Displaces volume already accounted for in swing engine cavity
[9] Displaces volume already accounted for in swing engine covers
[10] Assumes replacement of active intake valves with simple flipper valves.

Table 2. Current weight, volume, and power estimates for all major components of a 20W palm-sized MICSE power generation system, showing achievable values based on realistically foreseeable extensions of the current state-of-the-art.

characteristics of the proposed system could be determined. Note that the system produces 37.2 W of mechanical power at 21.9% thermal efficiency, with a net electrical power of just over 20W based on a 65% assumed efficiency of the inductive alternator. Such a four-stroke system would require small, fast, and lightweight active exhaust valves capable of surviving the high-temperature combustion products. Work is underway to develop valves meeting these requirements. Concurrently with this, a two-stroke MICSE system is being developed that will allow palm-sized power generation even if the development of such valves fails. Such a two-stroke system is shown in Fig. 12.

There are a number of competing system tradeoffs between a two-stroke and a four-stroke MICSE system. These include the inherent reduction in (nominal) thermal efficiency of a two-stroke cycle, since the exhaust ports open earlier in the cycle. However, this must be compared with the higher combustion temperatures and pressures made possible by near-stoichiometric operation of the two-stroke engine; *i.e.*, at air-fuel equivalence ratios near unity. Since fuel vapor and air are inductively pre-mixed outside the engine, the MICSE engine can be successfully operated at equivalence ratios closer to stoichiometric than is possible for traditional large-scale two-stroke engines, for which fuel-air mixing becomes a limiting factor. Note also that the comparatively high unburned hydrocarbon (UHC) emissions traditionally associated with two-stroke engines are not relevant to such a fully premixed MICSE system. Wall quench layer thicknesses within the combustion chambers of the 20W MICSE system remain negligibly small in relation to the chamber dimensions; for true "micro" scale engines operating at much lower power levels this can become a limiting factor. Moreover, the two-stroke MICSE system has two power strokes per cycle, and thus can be designed with a smaller and lighter engine core than a four-stroke system. The increased power density permits the

system to be used in applications where the fixed weight of the engine itself is a limiting factor, such as in certain MAV and UAV applications. The reduction in engine core weight also allows the shaft-coupled inductive alternator to be combined with a supercharger, as shown in Fig. 13. In this case, the inductive alternator is integrated in the supercharger, where the temperatures are low enough to allow the permanent magnets to retain their magnetic properties; such magnetic degradation typically begins around 300 C, well before the Curie temperature is reached. The supercharger boosts the thermal efficiency of the cycle and at the same time acts as an inductive pump for the fuel-air premixing system. The resulting net effect of such a two-stroke design is currently being assessed with an extension of the MICSE system performance model that includes such a coupled supercharger, however it currently appears that the net efficiency may actually be higher than with the four-stroke cycle.

The current palm-scale MICSE design incorporates the smallest currently-available commercial check valves for the intake side, for which temperatures remain comparatively low. The mass of these valves is just 0.3 g each, and they have a cracking pressure of 1 psi and working pressure up to 8000 psi.

Another key technology area for the palm-scale MICSE system is development of microignitors that can survive the in-chamber conditions over long period of time. Figure 14 shows our current technology for such microignitors. These are fabricated from commercially-available 790 μm-diameter ceramic rods (thermocouple insulators) with two integral channels. These channels each contain 125 μm tungsten filaments separated by 450 μm. The resulting small spark gap allows the spark voltage to be kept low enough that the ignition control circuit can use small integrated switching circuits as opposed to comparatively large high-voltage relays. The required spark energy to achieve ignition is of the order of 750 μJ/spark, and is controlled via the spark duration by the ignition control circuit. These microignitors are integrated in the engine core design so that the inflow of fresh fuel-air mixture scavenges the ignitor tips, increasing the reliability of ignition. Tests are currently underway to check for oxidation of the tungsten filaments over long-duration firing.

A final key technology area involves design of a high-efficiency inductive alternator for mechanical-to-electrical power conversion from the rotationally oscillating swing engine shaft motion. An effective alternator design for such a system will likely be very different from the optimum for continuously rotating systems. This is being done with state-of-the-art electromagnetic simulation software, which allows arbitrary inductor geometries, magnetic material properties, coil winding properties, load resistance, etc. to be specified, and includes effects of eddy currents and magnetic saturation on the alternator performance. The simulations predict the resulting electromagnetic field properties throughout the alternator, as well as the resulting induced current and voltage across the load resistance. An example of such a simulation is shown in Fig. 15 for a particular moving magnet design. The software being used for these simulations also permits parametric variations to be specified within the inductor design, thus allowing the oscillating frequency and angle of the swing-arm motion to specified, and results obtained for the induced voltage and current as a function of time. Results obtained to date indicate that 20W power output is possible with an integrated inductor sized to the palm-scale of the MICSE system.

7. Weight-Volume-Power Budgets

Table 2 gives current projections for the overall weight, volume, and power budget of the 20W small-scale MICSE system based on currently achievable component technologies for each of the system components. The table also gives realistically foreseeable values based on extensions of the current state-of-the-art. Values listed as achievable assume gains obtained from further miniaturization and integration of components, as well as elimination of certain components. The resulting power density and specific power available with such a palm-sized MICSE power generation system meets the goals for many of the applications listed in §1.

8. Conclusions

The MICSE system works on a different principle than other internal combustion approaches for power generation that have been considered to date. As a result, it has certain specific advantages over most other internal combustion-based approaches to power generation:

- The swing-arm creates four combustion chambers in a single base structure, with resulting mass and volume efficiencies that allow for lower weight and smaller size at the same power than linear piston approaches.

- Unlike linear free-piston approaches, the MICSE system has far lower vibration due to its use of a rotating swing-arm instead of a linearly translating piston.

- The swing engine is further unique among internal combustion systems in that it does not have any "dead points" in its operating cycle, and therefore starts readily with no external starter or manual priming.

- The swing motion produces excellent load-following characteristics; the system fully adjusts to large step changes in power demand in less than four swing cycles (0.05 sec).

- Load changes principally affect the swing angle rather than the swing frequency, permitting system components to operate over a narrow range of frequencies, providing for additional weight savings and increased reliability.

- The inherently fast system response time (0.05 sec) allows for virtually immediate on-demand startup and shutdown from the engine control circuit.

- Fabrication of the base cavity and swing arm use wire EDM to give part clearances below 10 μm, eliminating the need for seals between moving parts.

- The swing-arm maintains a constant optimal separation between the magnets and inductive coil to provide efficient coupling of mechanical power to electrical power.

- Engine control requires only simple four-state bit logic using threshold angular velocities obtained from the alternator output, and can be implemented in a chip without any mechanical linkage.

- Since timing control is based on the swing-arm position, the system automatically adjusts to changes in external load, equivalence ratio, and other operating factors.

In addition, work to miniaturize the original 65W MICSE 0 benchtop-scale system to a palm-scale 20W fully-integrated

power generation system has developed and demonstrated a number of key technologies that are crucial to the success of such an effort. Collectively, these indicate that such small-scale light-weight portable "micro" power generation systems may be able to successfully convert the high energy densities available in liquid fuels into electrical power for a number of emerging aerospace-related application areas requiring comparatively long-duration power sources in the 1W to 100W range.

References

Mijit, K. (2000) Design, analysis, and experimentation of a micro internal combustion swing engine. *Ph.D. Thesis*, The University of Michigan, Ann Arbor, MI.